

# MULTIOBJECTIVE OPTIMAL DESIGN OF PASSIVE AND HYBRID ACTIVE POWER FILTER BASED ON BACTERIAL FORAGING OPTIMIZATION ALGORITHM

S. MOLAEI      S. JALIZADE      M.MOKHTARIFARD  
E. E. Department, University of Zanjan, Zanjan, Iran , Sznu.molaei@gmail.com

**Abstract:** An optimal design method for passive power filters (PPFs) and hybrid active power filters (HAPFs) set at high voltage levels to improvements of Harmonic filtering and reactive power compensation is presented in this paper. To best study and vantage optimization multi objective optimization models for PPF and HAPF were used. In this paper, a bacterial foraging algorithm (BFA) aimed for solve the multi objective optimization problems for the designs of PPF and HAPF. The proposed algorithm is improved the reliability and practicability of the designed filters. For indicate performance and primacy of the proposed method, that results compared whit results of particle swarm optimization algorithm.

**Key words:** passive power filter; hybrid active power filter; bacterial foraging algorithm; harmonic compensation.

## 1. Introduction.

Recently power harmonic pollution due to nonlinear loads used in industry increased and they have many negative effects on power system equipment and customer, such as additional losses in overhead and underground cables, transformers and rotating electric machines, problem in the operation of the protection systems, over voltage and shunt capacitor, error of measuring instruments, and malfunction of low efficiency of customer sensitive loads. For this reason IEEE Standards provides a guideline for the limitation and mitigation of harmonics. Passive power filters (PPFs), active power filters (APFs) and hybrid active power filters (HAPFs) are used to attenuate this harmonics to an acceptable level [1, 2]. We can rate the power filters searching on several groups: harmonic estimation, power filters configuration and design, modulation and control method used to implement the compensation scheme. Therefore, recently a lot of research is being encouraged about the subjects: An algorithm for harmonic estimation is presented in [3]. It applied a particle swarm optimizer with passive congregation (PSOPC) to estimate the phases of harmonic components. A control algorithm for a hybrid power filter is proposed in [4]. In this paper control strategy is based on the dual formulation of the compensation system principles. Ref [5] proposes the use of conventional trial-and-error methods based on engineering experience for power filters design. The goal of design is to power filter's parameters which have better harmonics suppression effect and higher

capacity of reactive power compensation. Aiming at this problem, many optimization methods are introduced, such as genetic algorithm [6], simulated annealing [7], interaction multimodal genetic algorithm [8], particle swarm optimization [9], cultural algorithm [10], and chaotic evolutionary algorithm [11].  $\epsilon$ -constraint method [12], pareto-based methods are introduced, such as NSGA II[13]. Very methods treated the optimal design of power filters as a single objective problem. In fact, filter design should determine the optimal solution where there are multiple objectives. In this paper, optimal designs for both PPFs and HAPFs using an advanced bacterial foraging algorithm (BFA) are reported. For the optimal design of PPFs and HAPFs, the capacity of reactive power compensation, the original investment cost, and the total harmonic distortion (THD) were taken as the three objectives. The constraints included individual harmonic distortion, fundamental reactive power compensation, THD and parallel and series resonance with the system. A BFA-based algorithm was developed to search for the optimal solution. The numerical results of case studies comparing the BFA method and the PSO method are reported. From which, the primacy and availability of the BFA method and the designed filters are guaranteed.

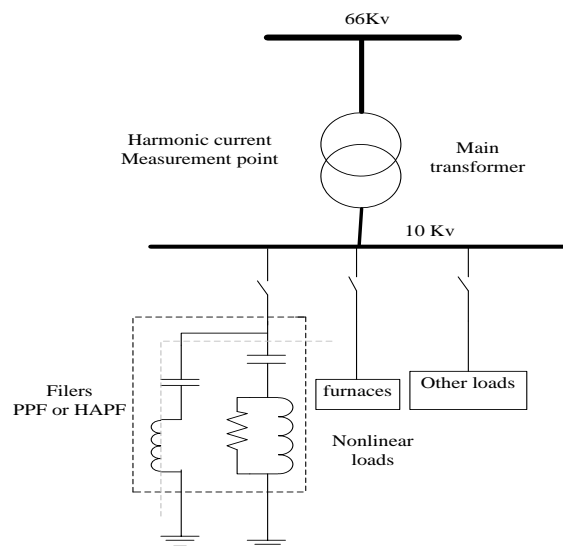


Fig. 2-1. Single diagram of system for case studies

## 2. Case study

Fig. 2-1 shows a system 10-kV 50-Hz with nonlinear loads, this system was selected to determine the optimal design for both PPFs and HAPFs. The nonlinear loads are the medium frequency furnaces commonly found in steel plants with opulent harmonic currents, especially the fifth and seventh orders, as shown in Table 1-1. The efficacy harmonic tolerances given in IEEE Standard 519-1992 and the Chinese National Standard GB/T14549-93 are listed in Table 1-1 as percentages of the fundamental current.

Table 1-1 shows that current THD, and the 5th, 23rd, and 25th order harmonic currents infringed the tolerances based on both standards. Also, the 7th and 11th order harmonics infringed the tolerance based on the National standard. Filters must therefore be installed to mitigate the harmonics sufficiently to satisfy both standards. PPF and HAPF are suitable for harmonic mitigation in such systems. For this system with nonlinear loads as medium frequency furnaces, the even and triple harmonics are very small and far below the standard values, so these harmonics are not considered. In addition, the harmonic voltages are in fact very small, so the voltages are aimed to be ideal. Table 1-2 shows that value related other quantities of system for case studies.

Table1-1  
harmonic current distributions in phase a and utility tolerances

Harmonic Order	Measured Value (%)	National Standard (%)	IEEE standard 519-1992 (%)
5	6.14	2.61	4
7	2.77	1.96	4
11	1.54	1.21	2
13	0.8	1.03	2
17	0.6	0.78	1.5
19	0.46	0.7	1.5
23	0.95	0.59	0.6
25	0.93	0.53	0.6
THD	7.12	5	5

Table1-2  
value related quantity of system for case studies

Parameter	value
fundamental current	1012 A
reactive power demands	3-4 M Var
short circuit capacity	132 MVA
equivalent source inductance	2.4 mH

## 3. Optimal design of PPFs

### 3-1. the principle of PPF

Passive power filter is an appropriate combination of capacitor, inductor and resistor. It has been divided into single-tuned filter, high pass filter and double-tuned filter, and so on. Because double-tuned filter is

complex in structure and difficult to tune, PPF usually consists of several single-tuned filters and a high pass filter in practice, which is showed in Fig.1. The characteristics of PPFs are detailed in [5, 16]. The single-tuned filters are used to filter the 5th and 7th order harmonics, while the high-pass damped filter is used to filter the 11th, 23rd, and 25th order harmonics.

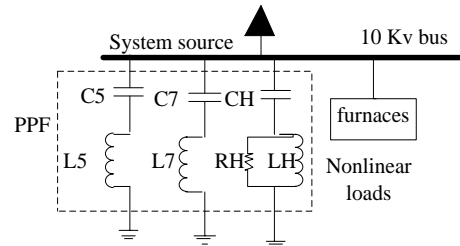


Fig.3-1. Typical structure of PPF

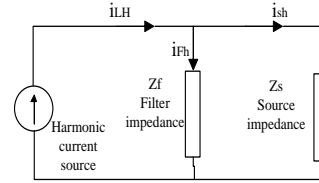


Fig. 3-2. Equivalent harmonic circuit model.

The resonant frequency and quality factor for a single-tuned filter can be expressed using:

$$F_i = \frac{1}{2\pi\sqrt{L_i C_i}}, i=5,7 \quad (1)$$

$$Q = \frac{\omega_i L_i}{R_i} = \frac{1}{\omega_i C_i R_i}, i=5,7 \quad (2)$$

Where  $\omega_i$  is the  $i$ th angular velocity. The characteristic frequency  $f_H$  and damping time constant ratio  $m$  for the high-pass damped filter are defined as:

$$f_H = \frac{1}{2\pi R_H C_H} \quad (3)$$

$$m = \frac{L_H}{R_H^2 C_H} \quad (4)$$

Fig. 3-2 shows Equivalent harmonic circuit model of Fig. 3-1. The nonlinear load is modeled as a harmonic current source, and the system source and PPF are modeled as impedance elements. The other loads will be neglected due to their very large impedance compared with the impedance of system source and the harmonic filter. Thus, the harmonic

current  $I_{sh}$  through the system source can be expressed using [17]:

$$I_{sh} = \left| \frac{Z_F}{Z_F + Z_S} \right| I_{Lh} \quad (5)$$

The harmonic order number is shown by  $h$  in (5).  $I_{Lh}$  is the  $h$ th order harmonic current produced by the nonlinear loads.  $I_{sh}$  is the  $h$ th order harmonic current to system source.  $Z_S$  and  $Z_F$  are the equivalent impedances of the system source and the PPF, respectively.

May be defined as the ratio of  $I_{sh}$  to  $I_{Lh}$  and defines the filtering performance of a PPF a harmonic attenuation factor  $\gamma$ : Advantage compensation performance can be obtained by decreasing the attenuation factor [17]. The attenuation factor is given by (6) in this case.

$$\gamma = \frac{I_{sh}}{I_{Lh}} = \left| \frac{Z_F}{Z_F + Z_S} \right| \quad (6)$$

### 3-2. Multiobjective Optimal Design Model for PPFs

The PPFs design is to determine the types, elements ( $R$ ,  $L$  and  $C$ ), set number, and parameters of filters to best satisfy the requirements of harmonic filtering and power factor improvement. In addition, the investment cost of PPF is taken into consideration in the design for constructing the filters with the lowest investment cost. These are formulated in an optimized model with some constraints and three objectives. Important objectives are constructed as follows at three section:

- 1) THD of source current minimize:

$$\min THD_I = \sqrt{\sum_{h=2}^N \left( \frac{I_{Sh}}{I_1} \right)^2} \quad (7)$$

$I_1$  is the rms value of the fundamental current and  $N$  is the highest harmonic order to be considered.

- 2) The initial investment cost Minimize:

$$\min F = \sum i_{5,7,H} = (K_1 C_i + K_2 L_i + K_3 R_i) \quad (8)$$

$k_1$ ,  $k_2$ , and  $k_3$  are cost weighting coefficients with respect to  $C$ ,  $L$ , and  $R$  [18].

- 3) The fundamental reactive power compensation Maximize. After installment of the PPF, the power factor of the system should be close to unity without overcompensation, so we have:

$$\max \sum i_{5,7,H} = Q_i \quad (9)$$

$Q_i$  is the fundamental reactive power afforded by the  $i$ th passive branch.

In continuation the constraints are constructed.

It should be noted that the tolerated harmonic levels of the IEEE standard are larger than those of the National standard, so the tolerated levels listed next are based on the National standard. Thus, both the IEEE and National standards are consented.

- 1) Needs of total harmonic filtering: The THD after compensation must meet the standards

$$THDI \leq THDI_{max} \quad (10)$$

where  $THDI_{max}$  is the tolerated level of THDI specified by the National standard.

- 2) Needs of individual harmonic filtering: Each order harmonic should satisfy the standards

$$I_{sh} \leq I_{hmax}, \quad h=5,7,11,13,17,19,23,25 \quad (11)$$

Where  $I_{hmax}$  is the tolerated level of the  $h$ th order harmonic current based on the National standard.

- 3) Fundamental reactive power compensation limits: The fundamental reactive power of filters must be restricted

$$Q_{min} \leq \sum_{i=5,7,H} Q_i \leq Q_{max} \quad (12)$$

Where  $Q_{min}$  and  $Q_{max}$  are limits of the total fundamental reactive power.

- 4) Series and parallel resonance restrictions: To avoid resonance with the system impedance, each filter is constrained to be inductive to the corresponding harmonics to be filtered. In addition, the resultant impedance of all filters must be inductive to those critical harmonics which may induce harmonic resonances in the system. The following inequality constraints are added to avoid resonance:

$$\text{Im}(Y_{sh}/Y_{5h}/Y_{7h}/Y_{Hh}) \neq 0 \quad (13)$$

$$\text{Im}(Z_{sh} + Z_{5h}/Z_{7h}/Z_{Hh}) \neq 0 \quad (14)$$

$h = 5, 7, 11, 13, 17, 19, 23, 25$

where  $\text{Im}()$  is imaginary part of a variable.  $Y_{Hh}$ ,  $Y_{5h}$ ,  $Y_{7h}$ , and  $Y_{sh}$  are the  $h$ th order harmonic admittances of the high-pass damped filter, the 5th single-tuned filter, 7th single-tuned filter, and source system, respectively.  $Z_{sh}$ ,  $Z_{5h}$ ,  $Z_{7h}$ , and  $Z_{Hh}$  are the  $h$ th order harmonic impedances of the high-pass damped filter, the 5th single-tuned filter, 7th single-tuned filter, and source system, respectively. When a filter branch has a fault, only this faulty branch is cut off, and the other branches should work normally. For example, when

considering an outage of the fifth single-tuned filter branch, the constraints are constructed as follows:

$$\text{Im}(Y_{sh}/Y_{7h}/Y_{Hh}) \neq 0 \quad (15)$$

$$\text{Im}(Z_{sh} + Z_{7h}/Z_{Hh}) \neq 0 \quad (16)$$

5) Constraints due to detuning effects: In before sections, filters are considered to be designed under normal conditions of the system. However, the parameters of practical systems vary. temperature and aging effects will alter the filter reactance and capacitance values. All these variations cause detuning problems. The constraints constructed to allow for the detuning effects are as follows.

a) When the system frequency rises to 50.5Hz or drops to 49.5Hz, the filtering performance of the PPF should still satisfy the standards listed in (10)–(16).

b) When the system impedance decreases by 20%, the filtering performance of the PPF should still satisfy the standards listed in (10)–(16).

c) In the worst case when the system impedance decreases by 20% and the system frequency is 50.5 Hz, the reactance and capacitance of each branch increase by 2% and 5%, respectively, but the filtering performance of the PPF should still satisfy the standards listed in (10)–(16).

d) When the capacitance of each branch increases by 5% and the reactance of each branch increases by 2%, the filtering performance of the PPF should still satisfy the standards listed in (10)–(16).

The PPF Designed in this method, will still have acceptable performance in most likely detuning situations. Although the PPF designed this way may not be the best one from the viewpoint of THD or other individual objectives, it will be the most useful one in practice, having a tradeoff between filtering performance and flexibility.

## 4. Optimal design of HAPF s

### 4-1. The principle of HAPF

The parallel HAPF has the advantages of easy installation and maintenance and can also be made just by transformation on the PPF installed in the grid. In order to demonstrate the optimal design method of HAPFs, an HAPF was designed and is shown in Fig. 4-1; it is supposed to be used in the same situation as that shown in Fig. 1-1. In this HAPF, an APF is used to improve the filtering performance and PPFs are mainly used to compensate for harmonics and reactive power [17]. The single-phase equivalent circuits of the HAPF, assuming that the APF is an ideal controllable voltage source  $V_{AF}$  and that the load is an ideal current source  $I_L$  shown by Fig. 4-2(a).  $V_{pcc}$  is the voltage of the

injected point,  $Z_F$  is the total impedance of the PPF,  $K$  is the controlling gain of the APF and  $Z_S$  is the source impedance. Fig. 4-2(b) shows the equivalent harmonic circuit. The harmonic attenuation factor  $\gamma$  and the harmonic current  $I_{sh}$  into the system source are given as follows:

$$I_{sh} = \left| \frac{Z_F}{K + Z_F + Z_S} \right| \quad (17)$$

$$\gamma = \frac{I_{sh}}{I_{Lh}} = \left| \frac{Z_F}{K + Z_F + Z_S} \right| \quad (18)$$

The voltage and current of APF can be derived as follows:

$$\dot{V}_{AP} = \sum_h V_{APh} = \sum_h -Z_{Fh} \dot{I}_{AFh} = \sum_h Z_{Fh} \dot{I}_{Lh} \quad (19)$$

$$\dot{I}_{AF} = \dot{I}_{AF1} + \sum_h \dot{I}_{AFh} \quad (20)$$

The rms value of  $V_{AF}$  is defined as

$$V_{AF} = \sqrt{\sum_{h=5,7,11,13,17,19,23,25} V_{APh}^2} \quad (21)$$

The APF capacity is determined by the current  $\dot{I}_{AF}$  and the voltage  $\dot{V}_{AF}$ . The low VA rating of APF can be achieved by decreasing  $\dot{I}_{AF}$  and  $\dot{V}_{AF}$ . In this shunt hybrid topology, the current  $\dot{I}_{AF}$  is almost constant, so decrease the voltage  $\dot{V}_{AF}$  is the only way to reduce the VA rating of APF.

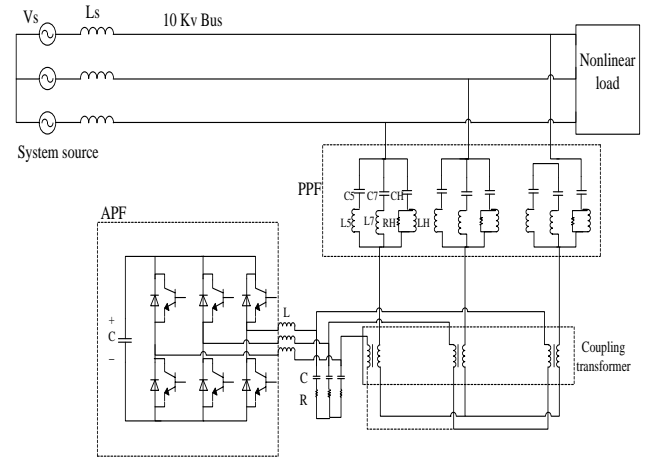


Fig. 4-1. Shunt HAPF.

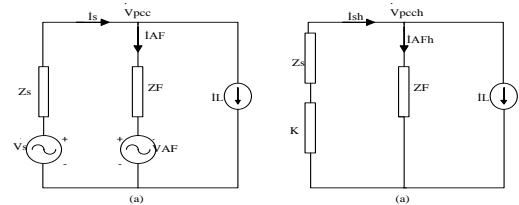


Fig. 4-2. Single-phase equivalent circuits of the HAPF. (a) Equivalent circuit. (b) Equivalent harmonic circuit.

## 5. Bacterial Foraging Optimization Algorithm

Bacterial Foraging optimization is based on foraging behavior of Escherichia coli (E.coli) bacteria present in the human intestine and been already implemented to real world problems [14]. BFA algorithm can be explained by four processes namely, chemo taxis, swarming, reproduction, and elimination-dispersal [15]. Below briefly described each of these processes.

### A-Chemotaxis:

This process simulates the swimming and tumbling movements of an *E. coli* cell by a set of rigid flagella. An *E. coli* bacterium can move in two different ways. It can swim for a period of time in the same direction or it may tumble, and alternate between these two modes of operation for the entire lifetime. This alternation between the two modes enables the bacterium to move in random directions and search for nutrients. Suppose,  $\theta^i(j,k,l)$  represents *i*-th bacterium at *j*-th chemotactic, *k*-th reproductive and *l*-th elimination dispersal step.  $C(i)$  is the run length which is a constant in basic BFA algorithm. In computational chemotaxis, the movement of the bacterium is represented as:

$$\theta^{i(j+1,k,l)} = \theta^i(j+1,k,l) + C(i)\Delta(i) / \sqrt{\Delta^T(i)\Delta(i)} \quad (22)$$

where  $\Delta$  indicates a vector in the random direction whose elements lie in  $[-1, 1]$ .

### B-Swarming:

It is always desired that when any one of the bacteria reaches the better location, try to attract other bacteria so that they reach the desired place more rapidly. The effect of swarming is to make the bacteria congregate into groups and move as concentric patterns with high bacterial density. Mathematically, swarming can be represented by

$$J_{cc}(\theta, P(j,k,l)) = \sum_{i=1}^S J_{cc}(\theta, \theta^i(j,k,l)) = \sum_{i=1}^S [d_{attractant} \cdot \exp[-w_{attractant} \sum_{m=1}^p (\theta_m - \theta_i)^2]] + \sum_{i=1}^S [h_{repellant} \cdot \exp[-w_{repellant} \sum_{m=1}^p (\theta_m - \theta_i)^2]] \quad (23)$$

$J_{cc}(h, P(j,k,l))$  is represents the objective function value to be added to the actual objective function (to be minimized) to present a time varying objective function,  $S$  is total number of bacteria,  $P$  is number of variables to be optimized, which are present in each bacterium,  $\theta = [\theta_1, \theta_2, \dots, \theta_p]$  is a point in the  $p$ -dimensional search domain.

$d_{attractant}$ ,  $w_{attractant}$ ,  $h_{repellant}$ ,  $w_{repellant}$  are different coefficients that should be chosen properly.

### C-Reproduction:

The least healthy bacteria eventually die while each of the healthier bacteria (each with the lower cost function) asexually split into two bacteria, which are then placed in the same location. Thus, the population size after reproduction is maintained constant.

### D-Elimination and dispersal:

A sudden or gradual change in the location where a bacterium population lives may occur due to noxious substance, the temperature rises abruptly in the area or some other influence. Events can kill or disperse all the bacteria in a region. This reduces the chances of convergence at local optima location. To simulate this phenomenon in BFA algorithm, some bacteria are chosen, according to a preset probability  $P_{ed}$ , to be dispersed and moved to another position within the environment.

The BFA algorithm parameters are denoted as  $p, S, N_c, N_s, N_{re}, N_{ed}, P_{ed}$ , where  $p$  is dimension of the search space,  $S$  is the total number of bacteria in the population,  $N_c$  is number of chemotactic steps,  $N_s$  is swimming length,  $N_{re}$  is number of reproduction steps,  $N_{ed}$  is number of elimination-dispersal events,  $P_{ed}$  is elimination-dispersal probability. The parameters selected for the proposed BFA algorithm are shown in Table 5-1.

It is certainly impossible to explore all the potential uses of BFA in this single article, but we briefly point to the some of them. It should seem at least plausible that there are applications of the methods to optimization, optimal control, adaptive estimation and control, and model predictive control.

Table 5-1  
Parameters of BFA algorithm.

parameter	S	$N_c$	$N_s$	$N_{re}$	$N_{ed}$	$P_{ed}$
value	10	30	4	5	4	0.25

## 6. Optimal Design for PPF and HAPE Based on BFA

In this paper, the capacitance of each branch of PPF and the characteristic frequency of the high-pass damped filter are chosen as optimal variables  $X_i = (C_5, C_7, C_H, f_H)T$ , while the tuning frequencies of the fifth and seventh single-tuned filters are predetermined as 242 and 342 Hz, respectively. According to the optimization objectives in (7)–(9), the corresponding fitness functions are as shown as:

$$F1(X) = THDI \quad (24)$$

$$F2(X) = F \quad (25)$$

$$F3(X) = \sum i_{5,7,H} = Q_i \quad (26)$$

Then, the optimal design of PPF is obviously a multi-objective optimization problem. The usually adopted method for multi-objective optimization is to construct a combinatorial fitness function by integrating all the objectives with linear weights, so

that the multi-objective optimization problem can be turned into a single objective optimization problem, which is much easier to deal with. However, the combinatorial fitness function has many extreme points, which tends to cause the optimal algorithm to fall into local minimums. This method will also cause unbalance between the different objectives. In order to overcome these disadvantages, an effective approach is adopted to solve this multi-objective problem, as explained in (27)–(29).

Among the three objectives, the most important objective, i.e., *THDI* is chosen as the final optimization objective, and the other two objectives are considered as “acceptable-level” constraints. These constraints are different from the common constraints referred to in (10)–(16)

$$\min F_1 \quad (27)$$

$$F_2 \leq \alpha_1 \quad (28)$$

$$\alpha_2 \leq F_3 \leq \alpha_3 \quad (29)$$

Where  $\alpha_1$ ,  $\alpha_3$ , and  $\alpha_2$  are the highest and lowest acceptable levels for the secondary objectives, respectively.

For HAPEs similar to PPF the corresponding fitness functions are defined as:

$$F_1(X) = V_{AF} \quad (30)$$

$$F_2(X) = THDI_{HAPF} \quad (31)$$

$$F_3(X) = \sum i_{5,7,H} = Q_i \quad (32)$$

The objective of minimizing the APF capacity is chosen as the final objective, while the other two objectives are solved by using acceptable level constraints, as shown in the following equations:

$$\min F_1 \quad (33)$$

$$F_2 \leq \alpha_1 \quad (34)$$

$$\alpha_2 \leq F_3 \leq \alpha_3 \quad (35)$$

Where  $\alpha_1$ ,  $\alpha_2$  and  $\alpha_3$  are the highest and lowest acceptable levels for the secondary objectives, respectively. The pseudo-code of the complete algorithm is presented below:

**[Step 1]** Initialize parameters  $p$ ,  $S$ ,  $N_c$ ,  $N_s$ ,  $N_{re}$ ,  $N_{ed}$ ,  $P_{ed}$ ,  $C(i)(i=1,2\dots S), \theta^i$ .

**[Step 2]** Elimination-dispersal loop:  $l=l+1$

**[Step 3]** Reproduction loop:  $k=k+1$

**[Step 4]** Chemotaxis loop:  $j=j+1$

[a] For  $i=1,2\dots S$  take a chemotactic step for bacterium  $i$  as follows.

[b] Compute fitness function,  $J(i, j, k, l)$ .

$J(i, j, k, l) = J(i, j, k, l) + J_{cc}(\theta^i(j, k, l), P(j, k, l))$

(i.e. add on the cell-to cell attractant–repellant profile to simulate the swarming behavior)

[c] Let  $J_{last} = J(i, j, k, l)$  to save this value since we may find a better cost via a run.

[d] Tumble: generate a random vector  $\Delta(i) \in \mathbb{R}^p$  with

each element  $\Delta_m(i), m=1,2,\dots,p$ , a random number on  $[-1, 1]$ .

[e] Move: Let

$$\theta^{i(j+1,k,l)} = \theta^{i(j,k,l)} + C(i)\Delta(i) / \sqrt{\Delta^T(i)\Delta(i)}$$

This results in a step of size  $C(i)$  in the direction of the tumble for bacterium  $i$ .

[f] Compute  $J(i, j+1, k, l)$  and let

$$J(i, j+1, k, l) = J(i, j, k, l) + J_{cc}(\theta^i(j+1, k, l), P(j+1, k, l))$$

[g] Swim

i) Let  $m=0$  (counter for swim length).

ii) While  $m < s$   $N$  (if have not climbed down too long).

• Let  $m=m+1$ .

• If  $J(i, j+1, k, l) < J_{last}$  (if doing better), let  $J_{last} = J(i, j+1, k, l)$  and let

$$\theta^{i(j+1,k,l)} = \theta^{i(j,k,l)} + C(i)\Delta(i) / \sqrt{\Delta^T(i)\Delta(i)}$$

And use this  $\theta^{i(j+1,k,l)}$  to compute the new  $J(i, j+1, k, l)$  as we did in [f]

• Else, let  $m = N_s$ . This is the end of the while statement.

[h] Go to next bacterium ( $i+1$ ) if  $i \neq S$  (i.e., go to [b] to process the next bacterium).

**[Step 5]** If  $j < N_c$ , go to step 4. In this case continue chemotaxis since the life of the bacteria is not over.

**[Step 6]** Reproduction:

[a] For the given  $k$  and  $l$ , and for each  $i = 1, 2, \dots, S$ , let

$$J_{health}^i = \sum_{j=l}^{N_c+1} J(i, j, k, l)$$

Be the health of the bacterium  $i$  (a measure of how many nutrients it got over its lifetime and how successful it was at avoiding noxious substances). Sort bacteria and chemotactic parameters  $C(i)$  in order of ascending cost  $J_{health}$  (higher cost means lower health).

[b] The bacteria with the highest  $J_{health}$  values die and the remain  $S_r$  bacteria with the best values split (this process is performed by the copies that are made are placed at the same location as their parent).

**[Step 7]** If  $k < N_{re}$ , go to step 3. In this case, we have not reached the number of specified reproduction steps, so we start the next generation of the chemotactic loop.

**[Step 8]** Elimination-dispersal: For  $i = 1, 2, \dots, S$  with probability  $P_{ed}$ , eliminate and disperse each bacterium (this keeps the number of bacteria in the population constant). To do this, if a bacterium is eliminated, simply disperse another one to a random location on the optimization domain. If  $l < N_{ed}$ , then go to step 2; otherwise end.

## 7. Simulation Result

### 7-1) PPF

The system shown in Fig.2-1 is used to study the PPF designs. The planning of the filters must satisfy the harmonic tolerance levels and the reactive power compensation requirements based on both IEEE and National standards. The cost weighting coefficients  $k_1$ ,  $k_2$ ,  $k_3$ ; reactive power compensation limits  $Q_{min}$ ,  $Q_{max}$ ;

and acceptable-level limits  $\alpha_1$ ,  $\alpha_2$ ,  $\alpha_3$  are listed in Table 7-1.

Table 7-1

Some parameters relating to PPF design

$k_1$	$k_2$	$k_3$	$Q_{min}$	$Q_{max}$	$\alpha_1$	$\alpha_2$	$\alpha_3$
2(pu/uF)	3(pu/mH)	5(pu/ $\Omega$ )	3Mvar	4Mvar	.95pu	3.7Mvar	4Mvar

Table 7-2

Some parameters relating to BFA algorithm

$Q_{MIN}$	$Q_{MAX}$	$\alpha_1$	$\alpha_2$	$\alpha_3$
3.2	4.18	0.93	3.8	4.18

Table 7-3

Design results of PPFs based on BFA and PSO

Design parameters	BFA	PSO
The 5 <sup>th</sup> single-tuned filter	$C_5=69.02, L_5=6.032, Q_5=60$	$C_5=65.48\mu F, L_5=6.61mH, Q_5=60$
The 7 <sup>th</sup> single-tuned filter	$C_7=21.12, L_7=14.33, Q_7=60$	$C_7=16.54\mu F, L_7=13.09mH, Q_7=60$
High-pass damped filter	$C_H=46.26, L_H=2.31, m=.5$	$C_H=41.98\mu F, L_H=2.12mH, m=0.5$

Table 7-4

Harmonic current distributions with and PPFs based on BFA and PSO methods

2)	Harmonic Order	BFA-method (%)	PSO-method (%)
3)	5	1.11	1.01
4)	7	0.61	0.58
5)	11	0.74	0.82
6)	13	0.26	0.32
7)	17	0.17	0.2
8)	19	0.16	0.15
9)	23	0.25	0.3
10)	25	0.22	0.29
11)	THD	1.41	1.54
Reactive power compensation		4.18	4Mvar
cost		0.894	0.917pu

Table 7-5

Harmonic current distributions with PPFs alone considering detuning effects

12)	Harmonic Order	BFA-method (%)	PSO-method (%)
13)	5	2.63	2.44
14)	7	1.48	1.36
15)	11	0.75	0.87
16)	13	0.31	0.36
17)	17	0.19	0.24
18)	19	0.16	0.18
19)	23	0.38	0.36
20)	25	0.24	0.35
21)	THD	2.88	3.01

The values of  $k_1$ ,  $k_2$  and  $k_3$  are suggested in [18] and the value of  $\alpha_1$  is normalized with respect to the investment cost (1.0 pu) of a PPF designed using PSO methods. The other parameters relating to the BFA algorithm are listed in Table 7-2.

The PPFs optimal parameters obtained through PSO and BFA techniques are listed in Table 7-3. The comparisons between the filtering performances of PPFs designed using the PSO method and using

the BFA method is shown in Table 7-4. As seen in this table, the total reactive power compensation via BFA technique is 4.18 Mvar while this value is reached 4 Mvar by PSO method. In this case, 4.5 % improvement is obtained using proposed BFA. In addition, 2.5% reduction in cost is reached compared to PSO method.

The simulation results based on field measurement data are listed in Tables 7-5, 7-7 to 7-

9. As seen in the table 7-5, the total harmonic distortion (THD) via BFA technique is 1.41 while this value is reached 1.54 by PSO method. In this case, 4.6 % improvement is obtained using proposed BFA.

As seen, all harmonic components and THD of currents fall within the tolerated levels listed in Table 1-1. The fundamental reactive power compensation also meets the demands. However, the filtering performance of the PPF designed using the BFA method is significantly better than that designed using the PSO method as shown in Table 7-4. Fig.7-1 shows the harmonic attenuation factors of PPFs based on the BFA method and on the PSO method and clearly shows the better harmonic attenuation performance of the PPF designed using the BFA method when compared with that designed using the PSO method. The harmonic attenuation factor defined in this paper has the same meaning as the normalized resultant impedance magnitude seen from harmonic source based on system impedance magnitude [18]. Fig.7-1 also shows that no other resonant point is found. Moreover, there are no harmonic currents at the critical point, and the harmonic currents near the critical point are under control. For this respect, it is impossible for the system studied to have resonance when filters are on line under normal conditions. when filters are on line under normal conditions. Table7-5 shows the filtering performance under the worst detuning conditions, as described earlier. In the case of the PPF designed using the method based on BFA, the current THD (2.88%) and each order harmonic current are still within the tolerated levels and with the PSO method, although the current THD (3.01%) is within the criteria and larger than that using the method based on BFA.

The results also verify the necessity of considering detuning effects during the design process rather than only considering them after finishing the design, as do some studies in the literature [5]. Fig.7-2 shows the harmonic attenuation factor of the PPF designed using the method based on BFA and considering the worst detuning effects, which is in accordance with the results in Table 7-5, and no resonance points are found. Based on field measurement data, some simulation tests were conducted using MATLAB/Simulink. The results of simulation are shown in Figs.7-3 and 7-4. Fig.7-3 shows that the original source current is distorted with abundant harmonics. With a PPF designed using the method based on BFA, Fig.7-4 shows that the compensated source current is close to a pure sine wave.

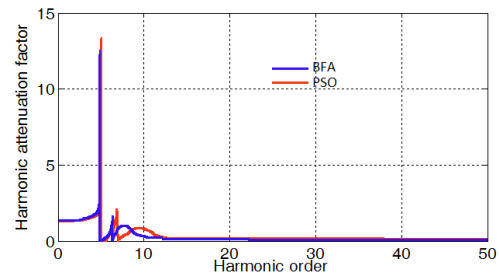


Fig. 7-1. Harmonic attenuation factors of PPFs. (blue) Harmonic attenuation factor of PPF based on the BFA method. (red) Harmonic attenuation factor of PPF based on PSO method.

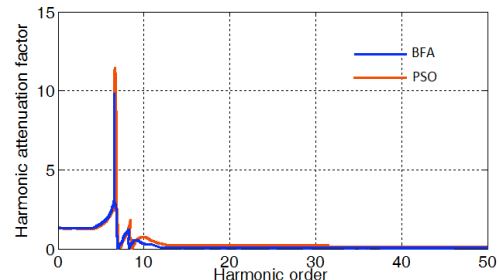
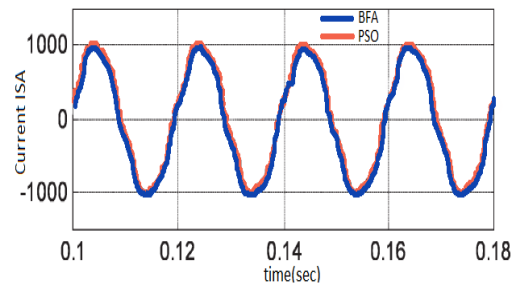
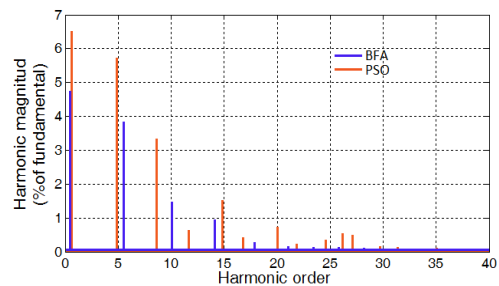


Fig.7-2. Harmonic attenuation factor of the PPF based on the BFA method (blue) -PSO method (red) with detuning effects.



(a)



(b)

Fig. 7-3 Original source current and its THD analysis without PPF(BFA method (blue) -PSO method (red)). (a) Original source current of phase A without PPF. (b) THD analysis of the original source current.



Table7-6

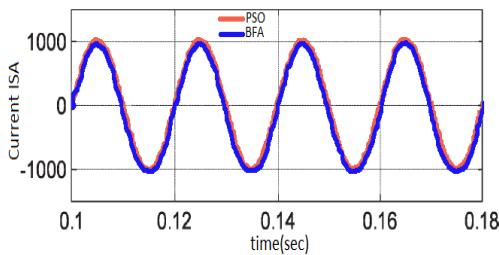
Design results of HAPFs based on BFA and PSO

Design parameters	BFA	PSO
The 5 <sup>th</sup> single-tuned filter	$C_5=57.04$ $L_5=7.39$ $Q_5=60$	$C_5=59.76\mu\text{F}$ $L_5=7.24\text{mH}$ $Q_5=60$
The 7 <sup>th</sup> single-tuned filter	$C_7=11.06$ $L_7=19.1$ $Q_7=60$	$C_7=12.326\mu\text{F}$ $L_7=17.58\text{mH}$ $Q_7=60$
High-pass damped filter	$C_H=55.1$ $L_H=1.15$ $m=.5$	$C_H=52.06\mu\text{F}$ $L_H=1.2\text{mH}$ $m=0.5$

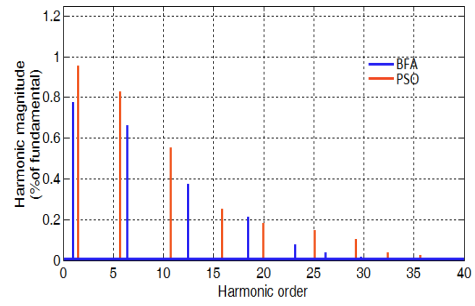
7-2) HAPE

The system in Fig. 1-1, with harmonics shown in Table 1-1, was studied for the HAPF design. The values of parameters  $Q_{\min}$  and  $Q_{\max}$  were the same as those in Table 7-1.

The parameters obtained BFA algorithm in Table 7-2. The gain  $K$  of the APF, as shown in Fig. 4-2, was selected as 20 [7]. The values of  $\hat{\alpha}_1$ ,  $\hat{\alpha}_2$  and  $\hat{\alpha}_3$  were set to 0.8%, 3.7 MVar, and 4 MVar, respectively. The HAPFs optimal parameters obtained through PSO and BFA techniques are listed in Table 7-6. The filtering performances of HAPFs based on BFA and PSO methods are compared in Table 7-7. It can be seen that the harmonic currents and reactive power are well compensated by both HAPFs and that the HAPF designed using the method based on BFA can obtain better filtering performance with lower THD (0.26%) and larger reactive power compensation (4MVar). Moreover, the voltage  $V_{AF}$  of the APF, in this case, was smaller than that based on PSO method. Therefore, the investment cost of the whole system is much reduced. Table 7-8 shows the harmonic current distributions when the PPF is working alone, without the APF. As seen in this table, the total harmonic distortion via BFA technique is 1.49 while this value is reached 1.68 by PSO method. In this case, 12 % improvement is obtained using proposed BFA.



(a)



(b)

Fig 7-4 Compensated source current and its THD analysis with PPF designed using the method based on BFA (blue) -PSO (red). (a) Compensated source current of phase A with PPF. (b) THD analysis of the compensated source current.

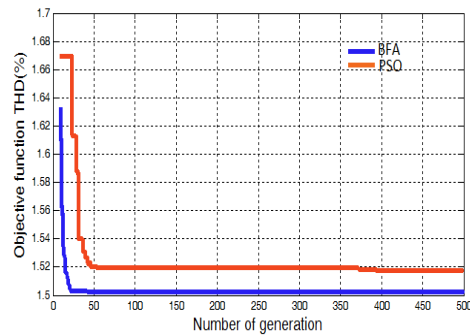


Fig-7-5 Convergence characteristics of BFA (blue) -PSO (red) for PPF design.

A comparison is made between the PSO method and BFA method, and it can be seen that all the harmonic currents and the THD are still within the standards, and the filtering performance of PPF based on BFA is a little better. In order to verify the filtering performances of HAPF and PPF alone under the worst detuning situations, comparisons are shown in Table 7-9. The filtering performance of PPF alone based on the BFA method is shown in Table 7-5. It is clear that both HAPFs, using BFA method and PSO method, can obtain excellent filtering performance in spite of detuning effects. When PPF runs alone without APF, the PPF using the BFA method can still mitigate all the harmonic currents and THD within the tolerance. The minimum fitness value evaluating process is depicted in Fig. 7-5 for PPF design. As it can be seen from the figure, the convergence of BFA is faster than PSO. This is because BFA algorithm provides the correct answers with high accuracy in the initial iterations which makes the responding time of this algorithm extremely fast.

Fig. 7-6 shows the harmonic attenuation factors of HAPF and PPF alone using The BFA design method and considering detuning effects. It can be seen that the harmonic currents are still well attenuated, and no resonance point can be found.

Table 7-7  
Harmonic current distributions with HAPFs based on BFA and PSO

Harmonic Order	BFA-method (%)	PSO-method (%)
5	0.32	0.24
7	0.31	0.24
11	0.22	0.25
13	0.09	0.1
17	0.065	0.07
19	0.05	0.06
23	0.1	0.13
25	0.1	0.13
THD	0.26	0.48
$V_{AF}$	101.23	116.64v
Reactive power compensation	4.18	4Mvar

Table 7-8  
Harmonic current distributions with HAPFs alone based on BFA and PSO methods

Harmonic Order	BFA-method (%)	PSO-method (%)
5	1.2	1.1
7	0.92	0.76
11	0.81	0.94
13	0.2	0.26
17	0.11	0.14
19	0.09	0.11
23	0.15	0.21
25	0.12	0.20
THD	1.49	1.68

Table 7-9  
Harmonic current distributions with HAPFs and PPFs alone considering detuning effects

Harmonic Order	BFA-method PPF (%)	BFA-method HAPF (%)	PSO-method HAPF (%)
5	2.68	0.71	0.65
7	1.91	0.82	0.75

11	1.03	0.19	0.23
13	0.36	0.09	0.1
17	0.18	0.06	0.08
19	0.14	0.05	0.06
23	0.23	0.1	0.14
25	0.23	0.1	0.14
THD	3.51	1.04	1.05

Furthermore, the attenuation factor of HAPF is much smaller than that of PPF, which shows the excellent harmonic mitigation performance of HAPF. The simulation using the MATLAB/SIMULINK software has been run based on field measurement data. The original source current without the HAPF is already shown in Fig.7-3, and the compensated source current with the HAPF is shown in Fig. 7-7. From Fig. 7-7, we can see that the source current is very close to a pure sine wave. Fig.7-8 shows the convergence characteristics of the BFA and PSO algorithm developed in this paper for optimal design of HAPF. In this paper, the PSO algorithm is run 200 times, and every time, it can converge within 50 iterations but BFA can converge within 26 iterations. All those can demonstrate the efficiency and validity of BFA for the optimal HAPF design.

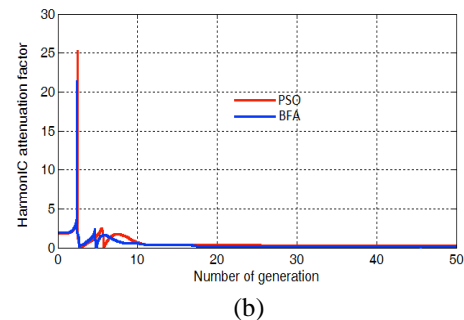
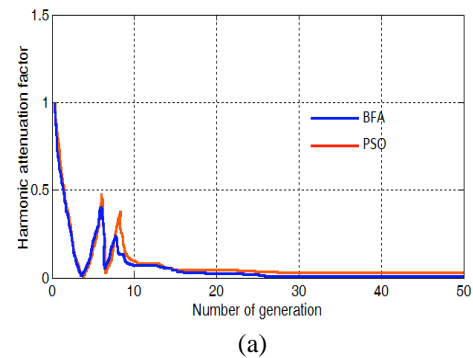
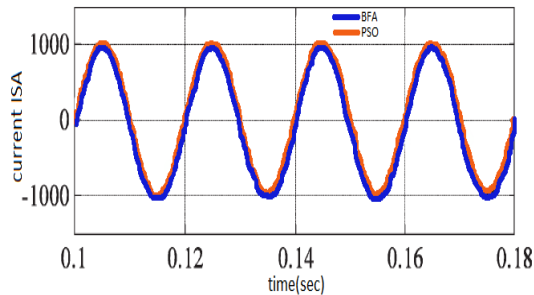
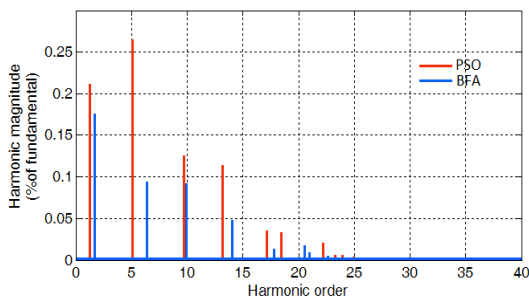


Fig. 7-6. Harmonic attenuation factors of the HAPF and its PPF alone based on the BFA (blue) -PSO (red)

method. (a) Harmonic attenuation factor of the HAPF based on the PSO method. (b) Harmonic attenuation of the PPF alone based on the BFA (blue) -PSO (red) method.



(a)



(b)

Fig. 7-7. Compensated source current and its THD analysis with HAPF based on the BFA (blue) -PSO (red) method. (a) Compensated source currents of phase A with HAPF.(b) THD analysis of compensated source current.

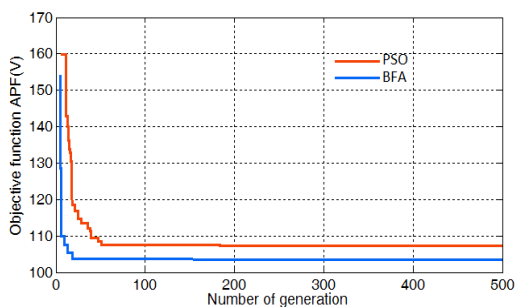


Fig. 7-8. Convergence characteristics of BFA (blue) - PSO (red) for HAPF design.

## 8. Conclusions

PPFs and HAPFs are the important devices for harmonic suppression of power network with harmonic source. Design of PPFs and HAPFs is to obtain a group of parameters including resistor, inductor and capacitor which meet the need of technology in each phase. A multiobjective optimal method based on BFA for the design of PPFs and HAPFs has been presented. A practical case with abundant harmonics was tested to demonstrate the

proposed method. The harmonic mitigation principles of both PPFs and HAPFs were explained, and a harmonic attenuation factor was defined to represent filter performance. An effective approach was adopted to turn multi-objective optimization problems into single objective problems, to simplify the solving process while retaining the characteristics of the multi-objective problem. Furthermore, the BFA approach to the optimal design of filters was introduced, from the simulation results and compared them with results of particle swarm optimization algorithm; the BFA was demonstrated to be very effective and suitable for the multiobjective optimal design of power filters.

## References

- [1] L. Asiminoaei, E. Aeloiza, P. N. Enjeti, and F. Blaabjerg, "Shunt activepower-filter topology based on parallel interleaved inverters," *IEEE Trans.Ind. Electron.*, vol. 55, no. 3, pp. 1175–1189, Mar. 2008.
- [2] Bhim Singh, Kamal Al-Haddad, Ambrish Chandra, "A review of active filters for power quality improvement" *IEEE Trans Indust Electron*,46 (5)(1999), pp. 960–971
- [3] Z. Lu, T.Y. Ji, W.H. Tang, Q.H. Wu, "Optimal harmonic estimation using a particle swarm optimizer" *IEEE Trans Power Deliv*, 23 (2)(2008), pp.1166–1174.
- [4] Patricio Salmeron, Salvador P. Litran, "A control strategy for hybrid power filter to compensate four-wires three-phase systems" *IEEE Trans Power Electron*, 25 (7) (2010), pp. 1923–1929
- [5] J. C. Das, "Passive filters-potentialities and limitations," *IEEE Trans. Ind. Appl.*, vol. 40, no. 1, pp. 232–241, Jan./Feb. 2004.
- [6] Zhao Shu-guang, Wang Yu-ping, Jiao Li-cheng, et al. Adaptive genetic algorithm based optimal design approach for passive power filters. *Proceedings of the Chinese Society for Electrical Engineering*, 7:173-176, 2004.
- [7] Zhu Xiao-rong, Shi Xin-chun, et al, Simulated annealing based multi-object optimal planning of passive power filters, In 2005 IEEE/PES Transmission and Distribution Conference & Exhibition, pages 1-5, 2005
- [8] He Na, Huang Li-na, Wu Jian, et al. Multi-objective optimal design for passive part of hybrid active power filter based on particle swarm optimization. *Proceedings of the Chinese Society for Electrical Engineering*, 12:63-69, 2008.
- [9] Li Shengqing, Zhu Yinghao, Zhou Youqing, et al. Optimal design of passive power filters based on interaction multi-modal genetic algorithm. *Transactions of China Electrotechnical Society*, 6:1-6, 2003.
- [10] Guo Yi-nan. Optimal Design of Passive power filters based on knowledge-based chaotic evolutionary algorithm. In *Proceedings of the 4<sup>th</sup> International Conference on Natural Computation*, pages 535-539, 2008.

- [11] Xiao Jian-hong, Peng Ke, Tu Chun-ming. Parameter design of passive power filter based on chaos optimization. *Converter Technology & Electric Traction*. 5:16-18, 2007.
- [12] Shuguang Zhao, Qiu Du, et al. UDT-based multi-objective evolutionary design of passive power filters of a hybrid power filter system. *Lecture Notes in Computer Science*. 4684:309-318, 2007.
- [13] Zheng Qiang, Lu Jiangang. Passive filter design based on non-dominated sorting genetic algorithm II. *Computer Measure & Control*. 15:135-137, 2007.
- [14] Dasgupta, S., Das, S., Abraham, A., Biswas, A., 2009. Adaptive Computational Chemotaxis in Bacterial Foraging Optimization: An Analysis. *IEEE Trans on Evolutionary Comp.*, vol. 13, pp. 919-941.
- [15] K. M. Passino, "Biomimicry of Bacterial Foraging for Distributed Optimization and Control," *IEEE Control Systems Magazine*, Columbus, Vol. 22, No. 3, 2002, pp. 52-67. doi:10.1109/MCS.2002.1004010
- [16] Y. P. Chang and C. J. Wu, "Optimal multiobjective planning of largescale passive harmonic filters using hybrid differential evolution method considering parameter and loading uncertainty," *IEEE Trans. Power Del.*, vol. 20, no. 1, pp. 408-416, Jan. 2005.
- [17] D. Rivas, L. Moran, J. W. Dixon, and J. R. Espinoza, "Improving passive filter compensation performance with active techniques," *IEEE Trans. Ind. Electron.*, vol. 50, no. 1, pp. 161-170 Feb. 2003.
- [18] C. J. Chou, C. W. Liu, J. Y. Lee, and K. D. Lee, "Optimal planning of large passive-harmonic-filter set at high voltage level," *IEEE Trans. Power Syst.*, vol. 15, no. 1, pp. 433-441, Feb.